Journal of Atmospheric and Solar-Terrestrial Physics 73 (2011) 1492–1499

Contents lists available at ScienceDirect

Journal of Atmospheric and Solar-Terrestrial Physics

journal homepage: www.elsevier.com/locate/jastp

Long-term variation of the semiannual amplitude in the aa index

Ana G. Elias [a,b], Virginia M. Silbergleit [a,c,*], Alicia L. Clua de Gonzalez [d]

[a] Consejo Nacional de Investigaciones Científicas y Técnicas, CONICET, Argentina
[b] Departamento de Física, Facultad de Ciencias Exactas y Tecnología, Universidad Nacional de Tucuman, Avenida Independencia 1800, 4000 Tucuman, Argentina
[c] INTECIN, Facultad de Ingeniería, Universidad Nacional de Buenos Aires, FIUBA, Avenida Paseo Colon 850-CABA, 1043 Buenos Aires, Argentina
[d] Divisão de Geofísica Espacial, Instituto Nacional de Pesquisas Espaciais, Avenida dos Astronautas, 1758, Jardim da Granja, 12227010, P.O. Box 515, São José dos Campos, São Paulo, Brazil

ARTICLE INFO

Article history:
Received 16 March 2010
Received in revised form
26 September 2010
Accepted 2 December 2010
Available online 21 December 2010

Keywords:
Geomagnetic activity
Semiannual variation

ABSTRACT

The long-term variation of the semiannual amplitude in the geomagnetic activity index aa is analyzed with the purpose of contributing to the understanding of solar variability, directly linked to geomagnetic variability. The time series of the semiannual oscillation amplitude, obtained through a wavelet analysis of the daily aa series, presents a long-term variation similar to that shown by solar and geomagnetic indices, like aa itself or Dst. However, the maximum in the semiannual amplitude series occurs around 1947, almost 10 years before it occurs in solar and geomagnetic indices time series. The phase of the semiannual oscillation fluctuates around the values predicted by the equinoctial and Russell–McPherron models, with a predominance of the equinoctial mechanism during the period of maximum semiannual amplitude. A possible source of changes in the equinoctial mechanism would be the secular variation of the Earth's dipole tilt. But, since it does not follow the semiannual amplitude trend, at first sight, it seems not to be responsible for the equinoctial predominance around 1947. The analysis of quiet and disturbed days separately indicates that only disturbed days present the semiannual annual amplitude maximum around 1947, so the 10 year time shift could be due to the mechanism responsible for the semiannual variation in geomagnetically active periods.

1. Introduction

The study of periodicities in solar data has long been of interest, being fundamental for understanding the mechanisms of solar variability and solar–terrestrial relationships. In general, frequency and amplitude of solar periodicities are not constant in time, that is solar and geomagnetic activity parameters present non-stationary oscillations. There are many studies dealing with trends in geomagnetic indices (Demetrescu and Dobrica, 2008; Rouillard et al., 2007; Cliver et al., 2002; Vennerstrom, 2000; to mention a few) but not so many dealing with trends in amplitude and phase of the known oscillations in solar and geomagnetic activity parameters. Among the latter, Le Mouel et al. (2004a, b) have analyzed the 6-month line amplitude of the aa index and obtained a long-term variation that they found similar to the long-term variation of various solar and magnetic parameters.

The well known semiannual variation in geomagnetic activity with maxima near equinoxes is not attributed to a conclusive origin but generally to one or more of the three following principal sources:

(1) The axial hypothesis caused by the annual variation of the heliographic latitude of the Earth, Bo (Cortie, 1912): the Sun's equator is inclined at an angle of about 7.3° with respect to the ecliptic (plane of the Earth's orbit), so Bo, which is the latitude of the Earth referred to the solar equator in degrees, varies with the epoch of the year. The two planes intersect at two points, which the Earth passes on about 5 June and 5 December (Julian days 156 and 339, respectively). On these dates the Earth is in the plane of the Sun's equator and Bo becomes nearly zero. On about 5 March and 5 September (Julian days 64 and 248, respectively) the Earth is at its maximum angular distance from the solar equatorial plane ($Bo = \pm 7.3^\circ$) and thus more closely aligned with active regions and mid-latitude coronal holes. The time variation of the geomagnetic effect follows the minus cosine of Bo (black line in Fig. 1), so, the cosine has its maximum value when $Bo = 0$ corresponding to the Earth aligned with the Sun's equator. Evidences of this mechanism were shown by Priester and Cattani (1962); and more recently, but acting with the contribution of the other two mechanisms described ahead, by Cliver et al. (2004) for example.

* Corresponding author at:INTECIN, Facultad de Ingeniería, Universidad Nacional de Buenos Aires, FIUBA, Avenida Paseo Colon 850-CABA, 1043 Buenos Aires, Argentina.
E-mail address: vms10ar@yahoo.com.ar (V.M. Silbergleit).

1364-6826/$ - see front matter © 2010 Elsevier Ltd. All rights reserved.
doi:10.1016/j.jastp.2010.12.001

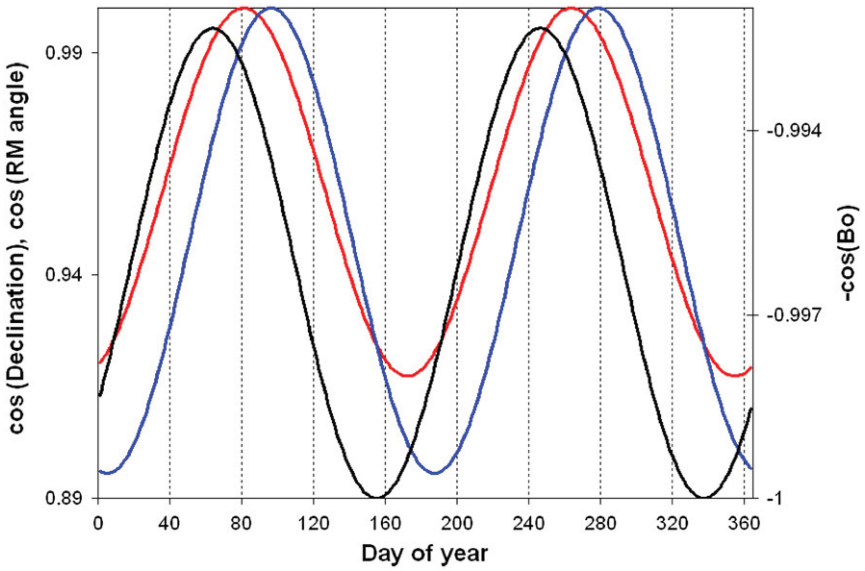

Fig. 1. Cosine of the heliographic latitude of the Earth, Bo, (black line), cosine of the declination (red line), and cosine of the sum Bo+declination (blue line), which represent the time variation of the effect on geomagnetic activity of the axial, equinoctial, and Russell–McPherron mechanisms, respectively, with the pair of maxima during 5 March–5 September, 21 March–21 September, and 5 April–8 October for each mechanism. Note: Bo was obtained from the Astronomical Almanac 2009 (available at http://asa.usno.navy.mil). (For interpretation of the references to color in this figure legend, the reader is referred to the web version of this article.)

(2) The equinoctial hypothesis caused by the annual variation of the orientation of the Earth's magnetic axis relative to the Earth–Sun line, ψ (Bartels, 1932; McIntosh, 1959; Svalgaard, 1977): geomagnetic activity maximizes at the equinoxes (March 21 and September 21, corresponding to Julian days 80 and 264, respectively) when the angle between these two orientations is 90° (declination=0) and the coupling efficiency with the magnetosphere should be maximum. Qualitatively, this is due to the Earth's magnetic field seen by the solar wind that is weakest when $\psi=90°$ (Svalgaard, 1977). The seasonal variation of ψ follows the variation of the declination and its effect on geomagnetic activity follows the cosine of the declination angle (red line in Fig. 1).

(3) The Russell–McPherron mechanism (Russell and McPherron, 1973): the controlling parameter is the angle φ between the z-axis of the geocentric solar magnetospheric (GSM) coordinate system and the solar equatorial plane which can be obtained from the sum of Bo and ψ, so it depends on both, the tilts of Earth's dipole and the solar equatorial plane. It may be thought then as a combined axial and equinoctial hypothesis. When φ is minimum, which occurs on 5 April and on 8 October (Julian days 95 and 281 respectively), geomagnetic activity is expected to reach a maximum, because at these times a solar wind magnetic field lying entirely in the Sun's equatorial plane has its maximum projection on the z-axis of the GSM coordinate system. Magnetic reconnection between the solar wind magnetic field and the Earth's dipole field is expected then (Russell and McPherron, 1973; McPherron et al., 2009). As McPherron et al. (2009) wrote: "Reconnection drives internal flows in the magnetosphere and produces magnetospheric sub-storms responsible for geomagnetic activity." The expected seasonal variation in geomagnetic activity due to φ corresponds to that of the cosine of the sum of Bo and ψ (that behaves like the absolute value of the solar P-angle mentioned by Cliver et al. (2002) as the angle of the Russell–McPherron mechanism). In summing Bo to the effect of the Earth dipole tilt, the maxima are shifted from March 21 and September 21 to April 5 and October 8, respectively, as can be noticed in Fig. 1, where cos(Bo+declination) is depicted in blue.

Moreover, according to Clua de Gonzalez et al. (1993) these three mechanisms could be acting together. There is also another proposed cause, not analyzed here, that is solar illumination (Lyatsky et al., 2001; Newell et al., 2002).

In the present work, we analyze the long-term variation of the semiannual amplitude in the aa index, not only to contribute to the understanding of the mechanisms of solar variability, but also to the origin of the semiannual variation in geomagnetic activity.

2. Data analysis

Daily mean values of aa index provided by the National Geophysical Data Center (ftp://ftp.ngdc.noaa.gov) for the period January 1868–December 2006 were used. To study the time behavior of aa semiannual periodicity the wavelet power spectrum (WPS), which is commonly applied in geosciences, was calculated using the wavelet computational algorithm of Torrence and Compo (1998). The shape of the chosen wavelet function must present the general characteristics of the time series, which is being analyzed. If the time series presents abrupt variations, the Haar wavelet may be the most convenient, but if it has smoother variations, the Mexican Hat or the Morlet wavelet are more adequate. In our case, focused on amplitude changes, a complex smooth wavelet such as the Morlet wavelet is the most appropriate (Kumar and Foufoula-Georgiou, 1997), since it consists of a complex sine wave modulated by a Gaussian given by

$$\Psi_o(\eta)=\pi^{-1/4}e^{i\omega_o\eta}e^{\eta^2/2}$$

where η is a non-dimensional "time" parameter (related to the scale) and ω_o is a non-dimensional frequency. We have restricted our analysis to the period range 5–7 months, and according to our needs of time and frequency resolution we have chosen $\omega_o=20$. The wavelet transform of the discrete time series aa(t) is assessed as

$$W_n(s)=\sum_{n'=0}^{N-1}\mathrm{aa}(t_{n'})\Psi^*\left[\frac{(t_{n'}-t_n)}{s}\right]$$

where ψ^* is the complex conjugate of the normalized Morlet wavelet ψ_o, which is scaled (by varying the scale s) and translated (by t_n). The argument $(t_{n'}-t_n)/s$ corresponds to η, and N is the total number of data points, that is number of days in the period January 1, 1868–December 31, 2006 (=50769). The scale s (that is given in days in

this case) varies from an initial to a final value in order to include the desired interval of periodicities. s is transformed to period T in days through the following function:

$$T = \frac{4\pi s}{\omega_o + \sqrt{2+\omega_o^2}}$$

The WPS is defined as $|W_n(s)|^2$.

Fig. 2 shows the WPS of aa for the period range around the semiannual periodicity. A clear enhancement of the semiannual amplitude is noticed in the 1950s and also towards the 2000s although with less intensity.

From the WPS the time series of the semiannual oscillation amplitude is obtained. This time series corresponds to $|W_n(s)|$ averaged over s corresponding to periods between 5.6 and 6.4 month. In Fig. 3 we compare the semiannual amplitude series with the long-term variation of the index itself that is the 11-year running mean of aa index. The semiannual amplitude and aa present an increasing trend since the 1900s until around 1947 (date of maximum of solar cycle 18) and 1956 (middle of ascending phase of solar cycle 19), respectively, followed by a steep decrease until 1970 in both curves. An increasing trend continues until almost the end of the record in the case of the semiannual amplitude. In the case of aa there is a maximum in ~1985–1990, and a decreasing trend since then.

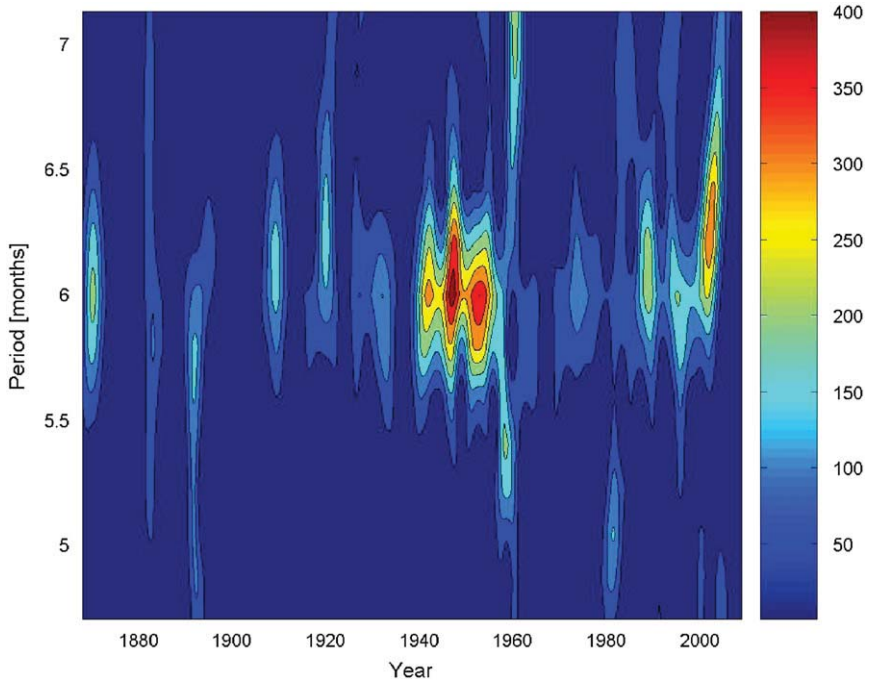

Fig. 2. Wavelet power spectrum (WPS) of aa for the period range 5–7 months assessed with the wavelet computational algorithm of Torrence and Compo (1998) using $\omega_o = 20$.

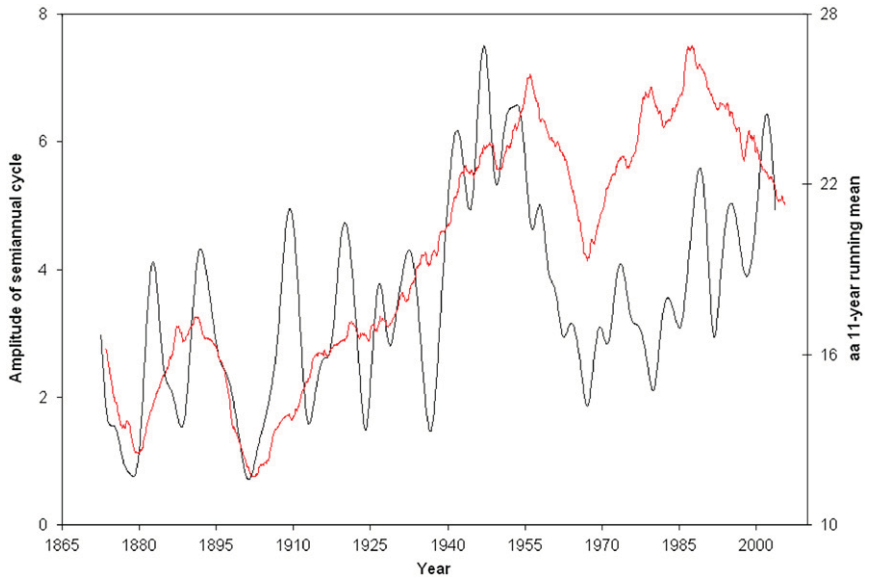

Fig. 3. Amplitude of the semiannual periodicity assessed from the wavelet power spectrum (black line), and 11-year running mean of aa index (red line). (For interpretation of the references to color in this figure legend, the reader is referred to the web version of this article.)

This analysis was repeated for quiet and disturbed days. For this purpose, the aa average over the five quietest days of each month was assessed, and also for the five most disturbed days. We called this monthly series obtained from the daily aa series, aaq and aad, respectively, which have now 1668 data points (number of months for the period January 1868–December 2006). The power spectrum of each monthly series was assessed, after a previous linear detrending. The semiannual oscillation appears in both series, as can be noticed in the normalized spectra depicted in Fig. 4, being more important and statistically significant in aad. The 95% and 99% confidence levels also shown in Fig. 4, are estimated as the 95th percentile value of the chi square distribution, χ^2, with two degrees of freedom, since the spectrum are normalized and the standard deviation equals one. The WPS of both series for the period range 5–7 months was estimated and plotted in Fig. 5a (aaq) and b (aad). The long term behavior of aad semiannual amplitude coincides with that of the semiannual amplitude of aa, as expected, considering that, on average, aad is around 7 times aaq. Fig. 6a and b shows the amplitude of the semiannual periodicity obtained from the WPS of aaq and aad, together with their respective 11-year

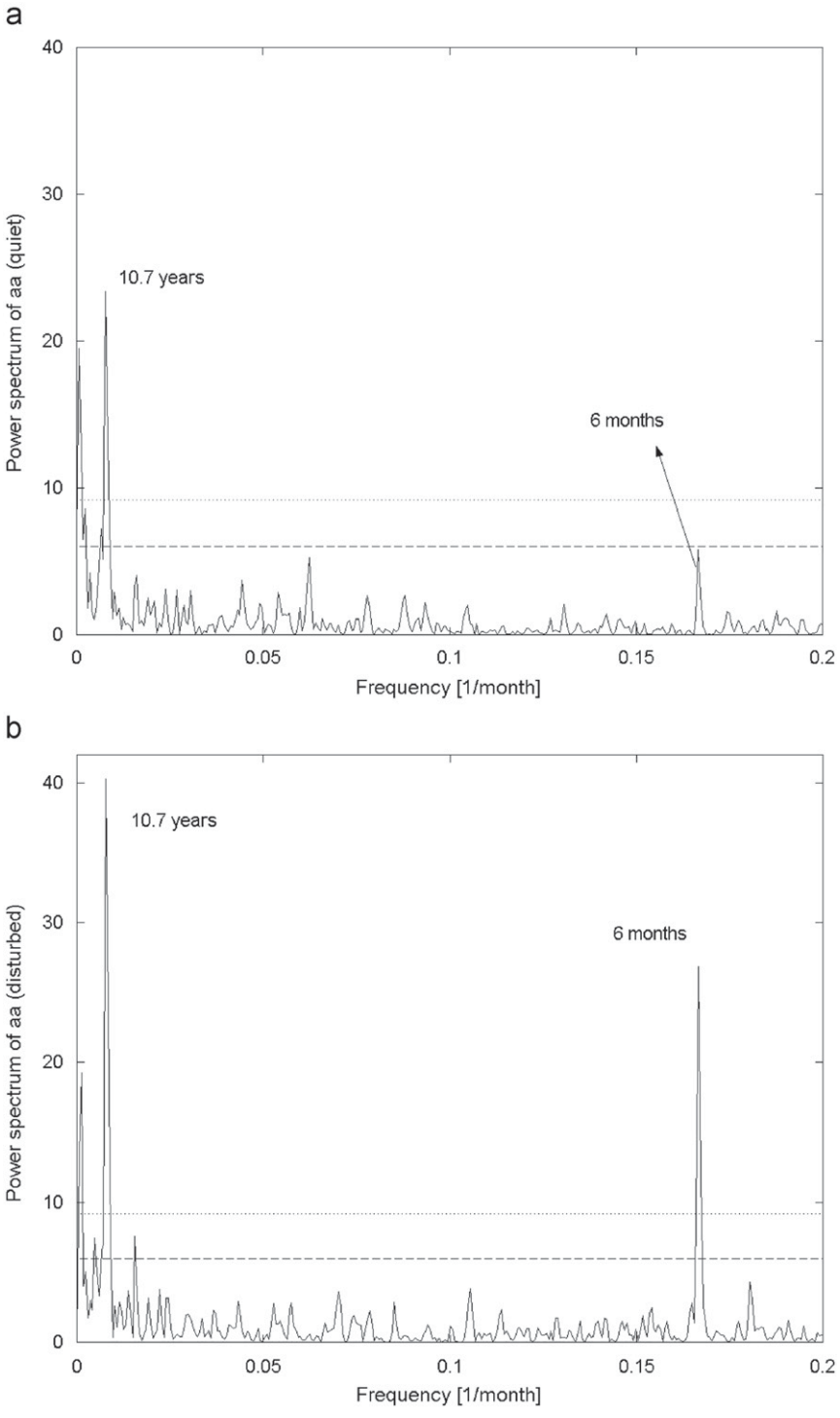

Fig. 4. Power spectrum of (a) aaq (aa average over the five quietest days of the month) and (b) aad (aa average over the five most disturbed days of the month). 95% (dashed line) and 99% (dotted line) significance levels.

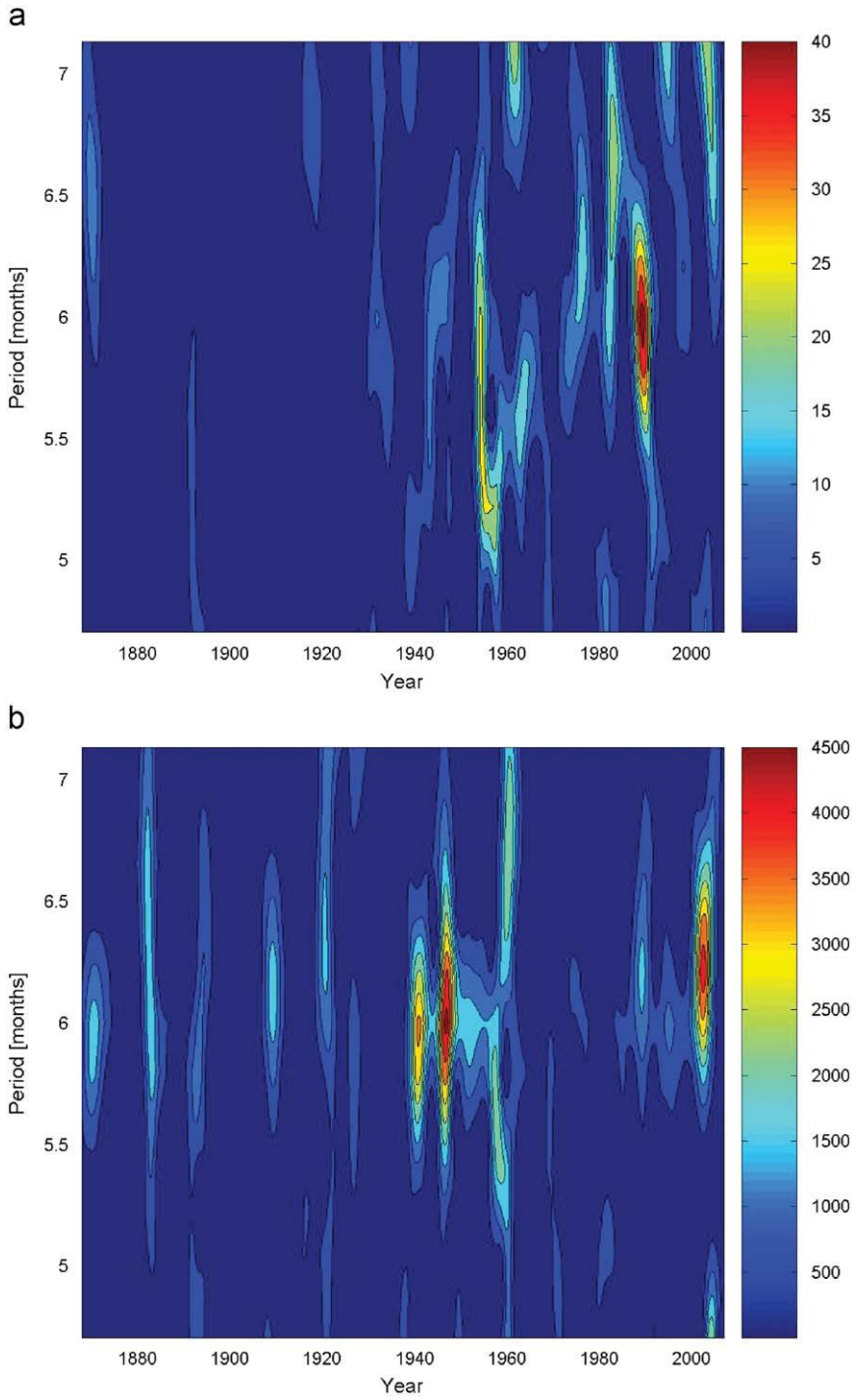

Fig. 5. Wavelet power spectrum (WPS) of aa for the period range 5–7 months assessed with the wavelet computational algorithm of Torrence and Compo (1998), using $\omega_o=20$, for (a) aaq (aa average over the five quietest days of the month) and (b) aad (aa average over the five most disturbed days of the month).

running averages (note that the scales of the axis corresponding to the amplitudes of the semiannual cycle for aad and aaq differ by a factor of 10). As can be seen in the figures, the long-term behavior of aaq and aad are very similar. However, this is not the case of the semiannual amplitude. For aaq, the long-term behavior of its semiannual amplitude follows the aaq trend.

Even the second enhancement in the semiannual amplitude coincides in time and relative magnitude with that of the 11-year running mean of aaq time series. But, for aad, as in the case of aa, the first strong enhancement occurs ~1947 previous to the peak of aad trend ~1956, and the second enhancement do not coincide, neither in time nor in magnitude. Historically, it is during cycle 19 (~1950–1960) that the number of geomagnetic storms reaches a maximum number (see e.g. Clua de Gonzalez et al., 2001).

The long-term variation of the phase of the semiannual oscillation was also analyzed. For each year of the analyzed interval the semiannual phase was estimated with the discrete Fourier transform. Then the computed values were smoothed by an 11-year running average. From the phase time series, the day of the first maximum was calculated and depicted in Fig. 7. This date mainly oscillates between March 21 (day of year=80) and April 5 (day of year=95) that correspond to the predicted first peak of the

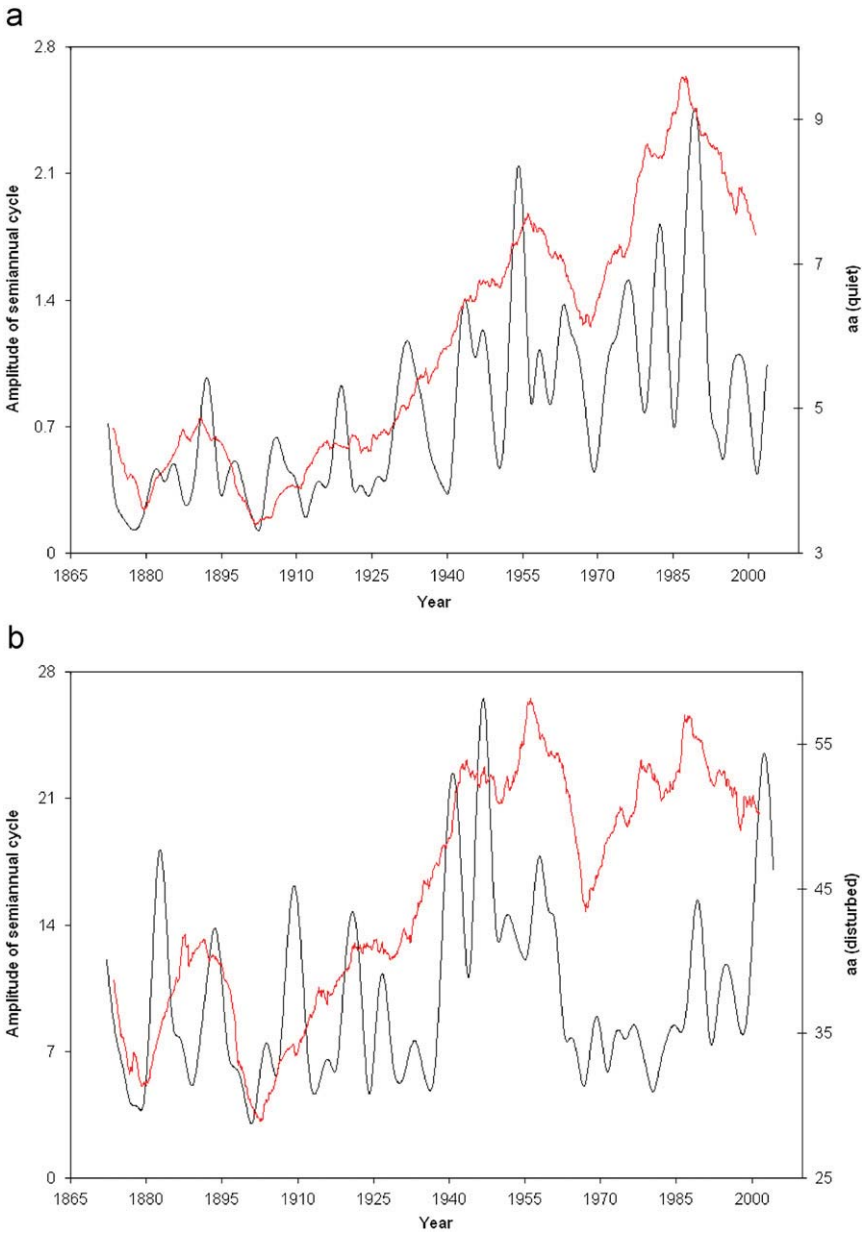

Fig. 6. Amplitude of the semiannual periodicity (black line) assessed from the wavelet power spectrum (black line), and 11-year running mean (red line) of (a) aaq and (b) aad. (For interpretation of the references to color in this figure legend, the reader is referred to the web version of this article.)

6-month oscillation by the equinoctial and Russell–McPherron models, respectively.

During the period of maximum amplitude (~1950 and indicated with an arrow in Fig. 7) the day of the first maximum oscillates closer to day 80, so it can be said that it corresponds to a predominance of the equinoctial mechanism of the semiannual variation, which, a priori, do not imply a reason for the semiannual amplitude enhancement at this time.

3. Discussion and conclusion

The long-term behavior of the semiannual amplitude in the aa index presents a maximum around 1947, almost ten years in advance of the maximum in aa long-term behavior, not in agreement with what we expected: enhanced semiannual amplitude coincident with stronger aa values (Lyatsky and Tan, 2003). This behavior is determined only by geomagnetic storms, since the semiannual amplitude of aa during quiet days is almost coincident with aa long-term behavior.

Our results are in agreement with Le Mouel et al. (2004a, b), and although they conclude that aa semiannual amplitude trend "has the characteristic shape of the curves representing the time averaged variation of various magnetic parameters", they obtain a maximum around 1950, which seems very close to the maximum found in the present work (see their figures 2 and 3).

According to Cliver et al. (2004), 1954 was a year with an "unusually strong semiannual variation of geomagnetic activity", not in agreement with our date of maximum semiannual amplitude. Although they selected this year based not only on the strength of the semiannual variation, but also on the degree of correlation with the angles associated with the three possible sources if semiannual variation, we made a comparison to show that through an analysis based only on amplitude, 1947 is a maximum. Fig. 8 shows the daily

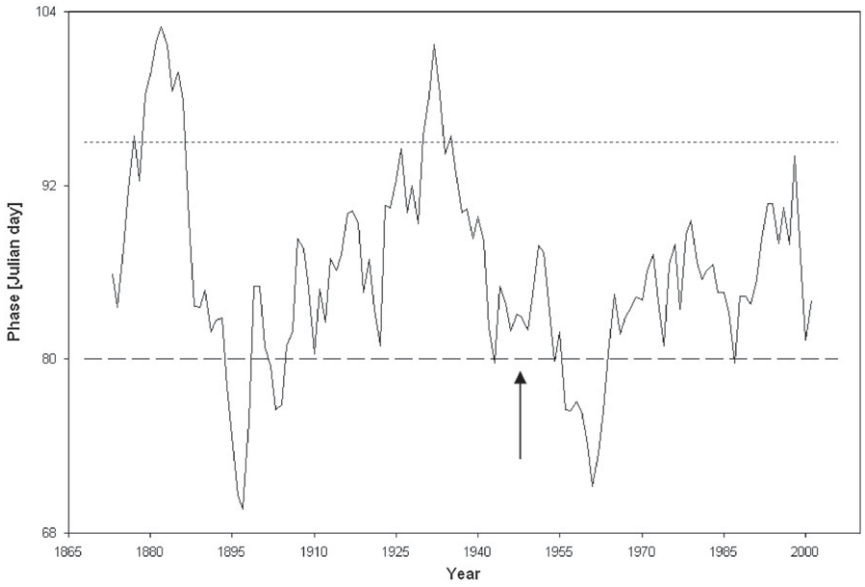

Fig. 7. Day of the first maximum of the semiannual variation assessed from semiannual phase, which was estimated for each year with the discrete Fourier transform and then smoothed with an 11-year running mean. March 21 (day-of-year = 80) (dashed line) and April 5 (day-of-year = 95) (dotted line). The arrow indicates the period of maximum amplitude.

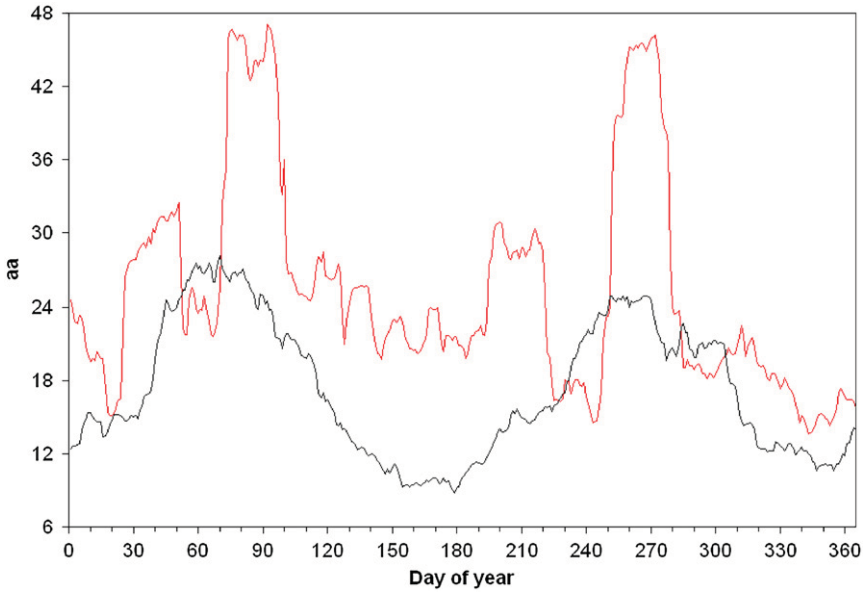

Fig. 8. Daily aa index for years 1947 (red line) and 1954 (black line) smoothed with a 25-day running mean. (For interpretation of the references to color in this figure legend, the reader is referred to the web version of this article.)

aa index for years 1947 (the year of maximum according to our results) and 1954, smoothed with a 25-day running mean. The amplitude obtained for 1947 is approximately 30 nT in comparison to the 20 nT value obtained for 1954.

During the period around 1947, according to the long-term behavior of the semiannual phase estimated here, there seems to be a predominance of the equinoctial mechanism of the semiannual variation. Since this mechanism is linked to the Earth's magnetic axis, we may think of a connection of its secular variation with the semiannual amplitude. However the dipole tilt secular variation that has decreased 1.2° between 1960 and 2005 after being nearly constant (Amit and Olson, 2008), does not seem to present the same pattern of the semiannual amplitude trend here detected.

The analysis of quiet and disturbed days separately indicates that only geomagnetic active periods present the semiannual annual amplitude maximum around 1947. We suggest then, that the 10 year time shift may be due to the mechanism responsible for the semiannual variation in geomagnetically active periods, which may be different from those of quiet periods.

The Russell–McPherron mechanism depends on properties of the solar wind that change with successive solar cycles in ways that could conceivably explain the variations in the amplitude of the semiannual oscillation. An examination of the seasonal rate of CME occurrence and the properties of the solar wind would be needed, but no data exist before 1964 to do this. With the help of proxies and deeper theory this can be pursued, and it will be the object of our future work. A deeper analysis remains then to be done together with the consideration of a non-linear relationship with the possible mechanisms responsible for the geomagnetic activity semiannual variation.

Acknowledgements

This work was partially supported by Facultad de Ingenieria, Universidad de Buenos Aires (PIP IN18) and CONICET (PIP 6540 and PIP 0470) of Argentina. The authors are grateful to P.A. Larocca for her kind collaboration. ALCG would like to thank the support of the "Fundo de Desenvolvimento Cientifico e Tecnologico" and the "Conselho Nacional de Desenvolvimento Cientifico e Tecnologico" (CNPq, Processo 342734/2008-2) of Brazil. The authors would also like to thank the NOAA's National Geophysical Data Center (NGDC) for the aa data.

References

Amit, H., Olson, P., 2008. Geomagnetic dipole tilt changes induced by core flow. Phys. Earth and Planet. Inter. 166, 226–238.

Bartels, J., 1932. Terrestrial-magnetic activity and its relation to solar phenomena. Terr. Magn. Atmos. Electr. 37, 1.

Cliver, E.W., Kamide, Y., Ling, A.G., 2002. The semiannual variation of geomagnetic activity: phases and profiles for 130 years of aa data. J. Atmos. Sol. Terr. Phys. 64, 47–53.

Cliver, E.W., Svalgaard, L., Ling, A.G., 2004. Origins of the semiannual variation of geomagnetic activity in 1954 and 1996. Ann. Geophys. 22, 93–100.

Clua de Gonzalez, A.L., Gonzalez, W.D., Dutra, S.L.G., Tsurutani, B.T., 1993. Periodic variation in the geomagnetic activity: a study based on the Ap index. J. Geophys. Res. 98 (A6), 9215–9231.

Clua de Gonzalez, A.L., Silbergleit, V.M., Gonzalez, W.D., Tsurutani, B.T., 2001. Annual variation of geomagnetic activity. J. Atmos. Sol. Terr. Phys. 63 (4), 367–374.

Cortie, A.L., 1912. Sunspots and terrestrial magnetic phenomena, 1898–1911: the cause of the annual variation in magnetic disturbances. Mon. Not. R. Astron. Soc. 73, 52.

Demetrescu, C., Dobrica, V., 2008. Signature of Hale and Gleissberg solar cycles in the geomagnetic activity. J. Geophys. Res. 113. doi:10.1029/2007JA012570.

Kumar, P., Foufoula-Georgiou, E., 1997. Wavelet analysis for geophysical applications. Rev. Geophys. 35, 385–412.

Le Mouel, J.-L., Blanter, E., Shnirman, M., 2004a. The six-month line in geomagnetic long series. Ann. Geophys. 22, 985–992.

Le Mouel, J.L., Blanter, E., Chulliat, A., Shnirman, M., 2004b. On the semiannual and annual variations of geomagnetic activity and components. Ann. Geophys. 22, 3583–3588.

Lyatsky, W., Newel, P.T., Hamza, A., 2001. Solar illumination as cause of the equinoctial preference for geomagnetic activity. Geophys. Res. Lett. 28, 2353–2356.

Lyatsky, W., Tan, A., 2003. Latitudinal effect in semiannual variation of geomagnetic activity. J. Geophys. Res. 108, 1204. doi:10.1029/2002JA009467.

McIntosh, D.H., 1959. On the annual variation of magnetic disturbance. Philos. Trans. R. Soc. London, Ser. A 251, 525.

McPherron, R.L., Baker, D.N., Crooker, N.U., 2009. Role of the Russell–McPherron effect in the acceleration of relativistic electrons. J. Atmos. Sol. Terr. Phys. 71, 1032–1044.

Newell, P.T., Sotirelis, T., Skura, J.P., Meng, C.I., Lyatsky, W., 2002. Ultraviolet insolation drives seasonal and diurnal space weather variations. J. Geophys. Res. 107. doi:10.1029/2001JA000296.

Priester, W., Cattani, D., 1962. On the semiannual variation of geomagnetic activity and its relation to the solar corpuscular radiation. J. Atmos. Sci. 19, 121–126.

Rouillard, A.P., Lockwood, M., Finch, I., 2007. Centennial changes in the solar wind speed and in the open solar flux. J. Geophys. Res. 112, 012130. doi:10.1029/2006JA012130.

Russell, C.T., McPherron, R.L., 1973. Semiannual variation of geomagnetic activity. J. Geophys. Res. 78, 92.

Svalgaard, L., 1977. Geomagnetic activity: dependence on solar wind parameters. In: Zirker, J.B. (Ed.), Coronal Holes and High Speed Wind Streams. Colorado Associated University Press, Boulder, CO, pp. 371.

Torrence, C., Compo, G.P., 1998. A practical guide to wavelet analysis. Bull. Am. Meteorol. Soc. 79, 61–78.

Vennerstrom, S., 2000. Long-term rise in geomagnetic activity—a close connection between quiet days and storms. Geophys. Res. Lett. 27, 69–72.